

X-RAY DIFFRACTION MEASUREMENTS FOR EXPANDED FLUID MERCURY

A substantial and continuous volume expansion from liquid to rarefied vapor occurs by the change of temperature and pressure around the liquid-vapor critical point without crossing the saturated vapor pressure curve. In the expansion process the mean interatomic distance increases by up to ten times compared with that under standard conditions. In metallic or semiconducting liquids, physical properties can drastically change. Liquid Hg, well known as a prototype of liquid metals, transforms into an insulating state when it is expanded up to the liquid-gas critical point (critical data of Hg [1]: $T_c = 1478\text{ }^\circ\text{C}$, $p_c = 1673\text{ bar}$, $\rho_c = 5.8\text{ g/cm}^3$). The first indication of the metal-nonmetal (M-NM) transition, which occurs around 9 g/cm^3 , was found in the electrical conductivity, thermoelectric power obtained by Hensel and Frank [2]. Many experimental and theoretical investigations focused on the M-NM transition have been made over the past few decades.

The information on the atomic arrangement of expanded fluid Hg is quite important for understanding the mechanism of the M-NM transition. However, the diffraction experiments for expanded fluid Hg are not easy because the critical pressure is very high. Tamura and Hosokawa [3] succeeded in measuring the X-ray diffraction pattern of expanded liquid Hg both in the metallic and critical regions using an in-house X-ray source.

We present new results of X-ray diffraction measurements using synchrotron radiation at SPring-8. These measurements extend from the liquid to the dense vapor region, which is beyond the liquid-vapor critical point.

Energy-dispersive X-ray diffraction measurements for expanded fluid Hg were performed using a diffractometer and high-pressure apparatus installed at the beamline **BL04B1**. White X-rays were used as the primary beam, and the scattered photons were detected by a solid state detector (SSD). The experimental conditions of high-temperatures up to $1520\text{ }^\circ\text{C}$ and of high-pressures up to 1765 bar were achieved with an internally heated high-pressure vessel made of a super-high-tension steel. Fluid Hg was contained in a single crystal sapphire cell.

Figure 1 shows the density isochores of fluid Hg plotted in the pressure-temperature plane [1].

Figure 2 shows the pair distribution function $g(r)$ for expanded fluid Hg under the different temperature and pressure conditions. To obtain the definite coordination number from the diffusive and broad atomic distribution in the non-crystalline state, we employed two different methods to integrate the first-neighboring atoms. In method **A**, $4\pi r^2 \rho_0 g(r)$ is integrated up to the maximum position of $g(r)$, r_1 , and doubled. Here ρ_0 denotes the average number density of Hg. In method **B**, $4\pi r^2 \rho_0 g(r)$ is integrated up to the first minimum position of $g(r)$, r_{\min} . We fixed r_{\min} as 4.5 in the entire density range because r_{\min} does not change so much except in the dense vapor region.

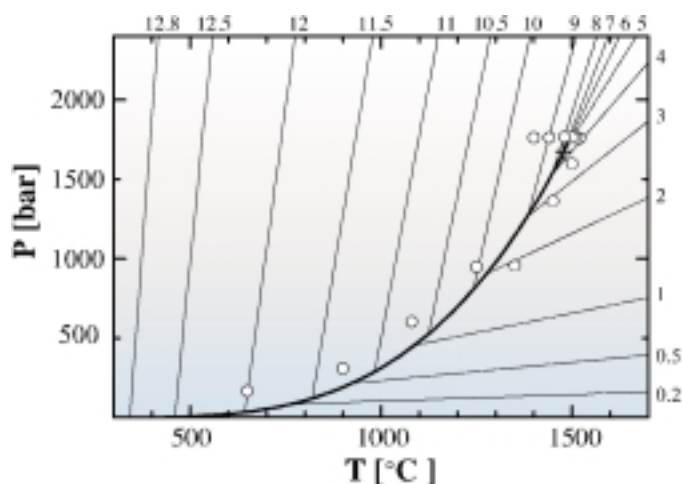


Fig. 1: Density isochores of fluid Hg plotted in the pressure-temperature plane [1]. Solid line indicates the saturated vapor-pressure curve and the cross shows the critical point. Open circles show the pressures and temperatures at which the X-ray diffraction measurements were performed [#].

The coordination numbers N_A and N_B obtained by methods **A** and **B** are plotted in Figure 3 as a function of density together with the nearest-neighbor distance r_1 at the bottom of the figure. N_B decreases substantially and linearly with decreasing density in the wide region from liquid to dense vapor. N_A also decreases almost linearly with decreasing density in the metallic region, but when the M-NM transition region is approached (*i.e.*, around 9-10 g/cm³), the deviation from the linear dependence appears. It seems that as the density deviation starts, the M-NM transition starts to occur.

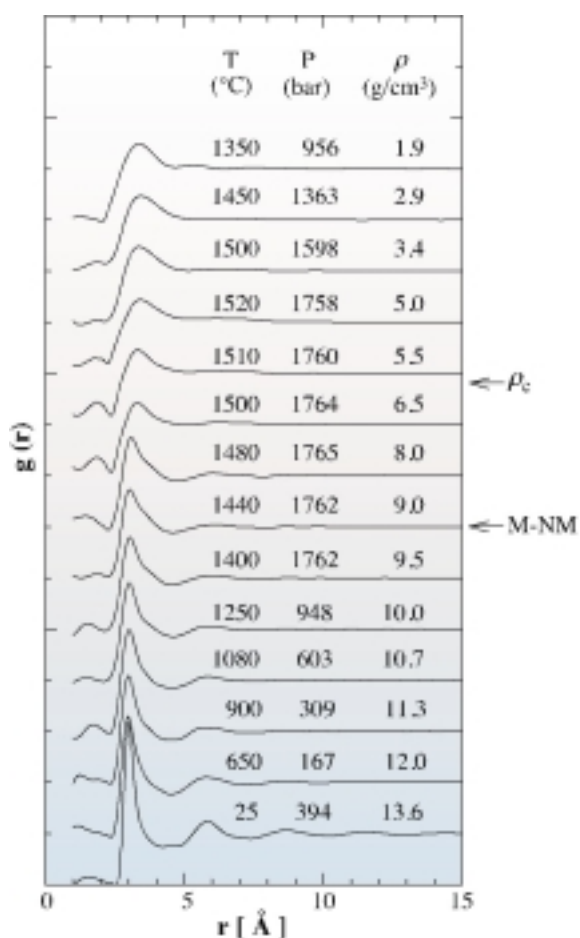


Fig. 2: Pair distribution function $g(r)$ for expanded fluid Hg. Temperature, pressure and density are indicated on the upper right hand side of each data plot [*].

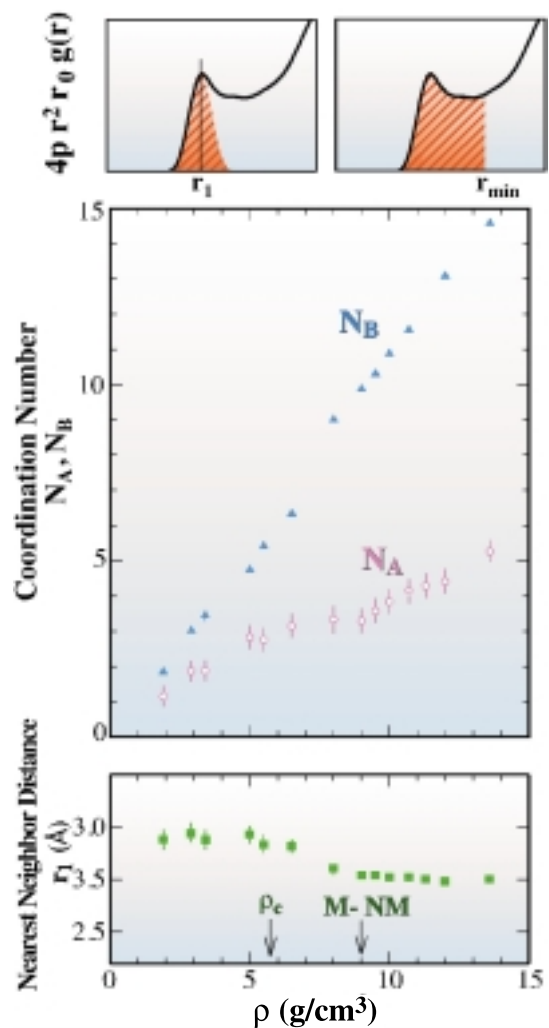


Fig. 3: Coordination numbers N_A , N_B and nearest-neighbor distance r_1 of expanded fluid Hg as a function of density. Circles and triangles denote N_A and N_B obtained using methods **A** and **B**, respectively. Squares show variation of r_1 [*].

In contrast to the N_A case, no anomalous behavior is observed in the behavior of N_B around this density region. In the dense vapor region the density variation of N_A changes again. As seen in the figure, r_1 in the metallic region remains almost unchanged with decreasing density, but when the M-NM transition region is approached r_1 starts to slightly increase. Such behavior coincides with that of N_A . In the dense vapor region r_1 substantially increases. The r_1 seems close to the interatomic distance of a Hg dimer in the rarefied vapor. From

these results, we can conclude that the density decrease of fluid Hg is essentially caused by the reduction of the coordination number through the entire density region as seen in the behavior of N_B . The variation in N_A gives more detailed information about the structural change accompanied by the M-NM transition. N_A represents the coordination number at the shortest distance in the first coordination shell, so the density variation of N_A suggests that the change in the nearest part of the first coordination shell is strongly related to the M-NM transition. As the most important observation, the gross feature of the density variation in N_A and r_1 in [Figure 3](#) suggests that there exist three different regions in the density: the metallic region from 13.6 to about 10 g/cm³, the M-NM transition region from 10 to the critical density of about 6 g/cm³ and the dense vapor region.

Kozaburo Tamura and Masanori Inui
Hiroshima University

E-mail: tamura@mls.ias.hiroshima-u.ac.jp

References

- [1] W. Gözlaff *et al.*, *Z. Phys. Chem. NF* **156** (1988) 219; W. Gözlaff, *Ph.D Thesis*, University of Marburg (1988).
 [2] F. Hensel and E. U. Frank, *Ber. Bunsenges. Phys. Chem.* **70** (1966) 1154.
 [3] K. Tamura and S. Hosokawa, *Phys. Rev. B* **58** (1998) 9030.
 [#] K. Tamura, M. Inui, I. Nakaso, Y. Oh'ishi, K. Funakoshi and W. Utsumi, *J. Phys. Condens. Matter* **10** (1998) 11405; [*] *Jpn. J. Appl. Phys., in press*.

CRYSTAL STRUCTURE ANALYSIS OF THE FULLERENE COMPOUNDS BY THE MAXIMUM ENTROPY METHOD

Alkali metal doped fullerenes in the form of A_2BC_{60} are fascinating substances. Many of them show superconductivity while a few others show no superconductivity. As the fundamental crystal structure, it is well known that C_{60} molecules form an fcc lattice and alkali metal atoms locate at both the tetrahedral and octahedral sites [1]. There is a close relation between the lattice constant of the compounds and their superconducting transition temperature, T_c [2,3]. For example, Rb_2CsC_{60} has a relatively high T_c . On the other hand, Li_2CsC_{60} shows no superconductivity.

It has been suggested that different bonding natures exist depending on their lattice constants and that they are closely related to the superconducting property [4]. Bonding nature may be divided into two regions, *i.e.*, the interatomic region between the doped metal atoms and the carbon-carbon region on C_{60} molecules. So far, there has been no definite experimental evidence on bonding nature. In this study, at the beamline **BL02B1**, the fine structure of Rb_2CsC_{60} and Li_2CsC_{60} are revealed [5], including the bonding nature for alkali metal doped fullerenes by the Maximum Entropy Method (MEM), which is an advanced imaging technique using diffraction data [6].

The MEM charge densities of Rb_2CsC_{60} and Li_2CsC_{60} are shown for a (110) plane in [Figures 1\(a\)](#) and [\(b\)](#), respectively. At a glance, it can be easily seen that there are distinct structural differences between Rb_2CsC_{60} and Li_2CsC_{60} . A non-superconducting alkali metal doped fullerene, Li_2CsC_{60} , has uniform charge densities of the C_{60} molecule due to nearly free rotation of C_{60} . In contrast, a superconducting alkali metal doped fullerene, Rb_2CsC_{60} , has some kinds of disorder. To visualize three-dimensional distributions of the charge on the carbon cage in Rb_2CsC_{60} , the MEM electron density distribution of C_{60} and Rb atoms are shown by an equi-contour surface at $2.0 \text{ e } \text{Å}^{-3}$ in [Figures 2\(a\)](#). In this figure, the characteristic features of the merohedral disorder, the hexagons facing toward Rb atoms and cloverleaf features,